JOURNAL OF Materials CHEMISTRY

The use of constant rate thermal analysis (CRTA) for controlling the texture of hematite obtained from the thermal decomposition of goethite

L. A. Pérez-Maqueda,[a] J. M. Criado,[a] C. Real,[a] J. Šubrt[b] and J. Boháček[b]

[a]*Instituto de Ciencias de Materiales de Sevilla, Centro Mixto Universidad de Sevilla-C.S.I.C., c/Américo Vespucio s/n, Isla de La Cartuja, 41092 Sevilla, Spain*
[b]*Institute of Inorganic Chemistry, Academy of Sciences of the Czech Republic, 25068 Rez, Czech Republic*

Received 9th February 1999, Accepted 4th June 1999

Constant rate thermal analysis (CRTA) has been used for studying the decomposition of three synthetic needle-shaped goethite samples. This method controls the reaction temperature such that the reaction rate and partial pressure of water vapour are kept constant at a selected value. The effects of the pressure of water vapour generated during the dehydration of goethite and of the decomposition rate on the porosity of the resulting hematite have been studied. The effect of the particle size of the precursors on the texture of the final products has also been analysed. By this method, acicular particles of α-Fe_2O_3 with controlled porosity oriented along the *c*-lattice axis (the long axis of the particle) have been prepared.

Introduction

The synthesis of nanosized α-Fe_2O_3 (hematite) is a matter of great interest because of the use of this material as ceramic humidity sensors,[1,2] catalysts,[3,4] pigments,[5] and as the raw material for the synthesis of γ-Fe_2O_3 (maghemite). This latter material has great technological importance as a ferrofluid and for its use in magnetic recording systems and magnetic pigments.[5–11]

It is well known[5,12] that maghemite is commonly synthesised through two consecutive steps of reduction and oxidation of hematite according to the following reactions:

$$\alpha\text{-}Fe_2O_3 \xrightarrow[H_2]{\approx 350\,^{\circ}C} Fe_3O_4 \xrightarrow[O_2]{\approx 350\,^{\circ}C} \gamma\text{-}Fe_2O_3 \qquad (1)$$

It has been reported in the literature[5] that the above reactions are topotactic, which means that maghemite retains the shape and size of the hematite used as its precursor. It is noteworthy that the crystallite size is not the only important factor influencing the properties of maghemite, but the particle shape is also a demanding factor for magnetic applications since it determines the shape anisotropy and then the coercive field value.[13] Acicular shaped particles of γ-Fe_2O_3 are required for longitudinal magnetic recording applications,[13,14] but the α-Fe_2O_3 precursor cannot be directly crystallised in such a shape. However, goethite (α-FeOOH) adopts this habit and can be transformed into hematite through the following reaction:

$$2\ \alpha\text{-FeOOH} \rightarrow \alpha\text{-}Fe_2O_3 + H_2O \qquad (2)$$

It has been reported[5] that the conversion of goethite into hematite is also a topotactic reaction and the size and shape of the starting material are preserved upon conversion into hematite. Thus, it can be concluded that goethite would be a suitable precursor for synthesising needle-shaped or lath-like crystals of hematite, magnetite or maghemite through the following sets of solid state reactions:

$$\alpha\text{-FeOOH} \rightarrow \alpha\text{-}Fe_2O_3 \rightarrow Fe_3O_4 \rightarrow \gamma\text{-}Fe_2O_3 \qquad (3)$$

Naono *et al.*[15,16] have shown that lath-like goethite crystals undergo topotactic dehydroxylation to porous α-Fe_2O_3 crystals, which retain the shape of the precursor. Many studies have been devoted to the elucidation of the formation of pores during the dehydroxylation of pure and substituted goethite.[17–21] The effects of several experimental parameters, such as annealing temperature and atmosphere, on the porosity have been studied. However, it must be pointed out that the calcination of goethite has been carried out under isothermal conditions or under a linear heating program until reaching the final annealing temperature selected. Neither of these two procedures allows one to discern the influence of the decomposition rate of goethite from the influence of the partial pressure of the water vapour generated on the porosity of hematite obtained. This is because the partial pressure of water vapour in the vicinity of the sample is expected to be proportional to the reaction rate at which it is generated from the thermal decomposition of goethite. For the two conventional methods mentioned above the reaction rate varies during the process depending on the experimental conditions used.

The scope of the present work is to analyse the influence of the particle size of a set of acicular goethite samples on their thermal stability and the texture of hematite obtained as the final product. The goethite samples used here were synthesised in a similar way in order to achieve the same purity for all the starting samples. The method of constant rate thermal analysis (CRTA) was used to monitor the thermal decomposition of goethite. This technique uses a feedback from the sample reaction itself to input into the algorithm governing the furnace control. Thus, the reaction temperature is monitored in such a way that both the reaction rate and the partial pressure of water vapour generated during the thermal dehydroxylation of goethite are maintained constant at the values selected by the user. This method allows one to distinguish between the influences of the particle size of the precursor and the partial pressure of water vapour on the texture and structure of the iron oxide obtained. The CRTA method has been previously used to control the texture and structure of some materials through kinetic control of the thermal decomposition of their precursors. The results reported here constitute the first attempt to use the CRTA method to control the texture and structure of the final products obtained from the thermal decomposition of goethite.

It is worthwhile noting that, as a result of the transformation of goethite into hematite, a non-uniform broadening of lines on the X-ray powder diffraction pattern has been previously reported.[15,22] This selective broadening was explained as a function of the generated porosity. The study of a series of

samples with different porosities here proposed would contribute to a better understanding of the reported XRD selective line-broadening of hematite obtained from goethite precursors. It would allow one to determine whether this non-uniform broadening is caused by the porosity, or by other factors like the lath-like morphology of hematite,[23] the twinned nature of the products[24] or an incomplete ordering of iron ions.[25,26]

Experimental

Synthesis of goethite

The preparation procedure consisted of the following steps: (i) a solution containing 250 g l^{-1} of $FeSO_4 \cdot 7H_2O$ was neutralised at room temperature with a 13.5 wt% NH_3 (aq) solution until a portion of the iron ions was precipitated (10% for G10, 25% for G25 and 100% for G100); (ii) air was bubbled through the dispersion until the pH of the dispersion dropped to *ca.* 4 and the colour turned from dark blue to yellow; (iii) the temperature was elevated to 60 °C and the pH value was maintained in the range 3.5–4 until all the Fe was precipitated; (iv) the yellow precipitate was then separated by filtration and washed with distilled water until no SO_4^{2-} was detected in the filtrate; (v) finally, the solid was dried at room temperature overnight.

Methods

Particles were examined by transmission electron microscopy (TEM) to analyse their size and shape as well as the size and shape of the pores. The crystalline structures of the solids were assayed by powder X-ray diffraction (XRD) with Cu-Kα radiation and a graphite monochromator. The dimensions of the crystallites were calculated from the broadening of the XRD peaks using Scherrer's equation. The specific surface area was determined by the nitrogen adsorption (single point BET) method.

To study the thermal transformation of the goethite samples into hematite, some experiments were carried out using a linear heating rate programme under vacuum and in static air. Another experiment was performed in a closed tube under the pressure of water vapour produced by the decomposition.

In addition, constant rate thermal analysis (CRTA) equipment developed in our laboratory (Fig. 1) was used to study this thermal transformation. In our CRTA equipment, the pressure gauge output is connected by an interface to the temperature controller so that the pressure above the sample (P) is kept constant at a selected value. The gas pressure can be controlled in the range from 10^{-5} to 10 Torr. Since the pressure of the gases generated in the reaction is proportional to the reaction rate (C), the reaction rate is also kept constant during the whole dehydroxylation process. This CRTA instrument allows variation of the reaction rate while keeping the water vapour pressure constant, by modifying the amount of sample or the pumping rate.

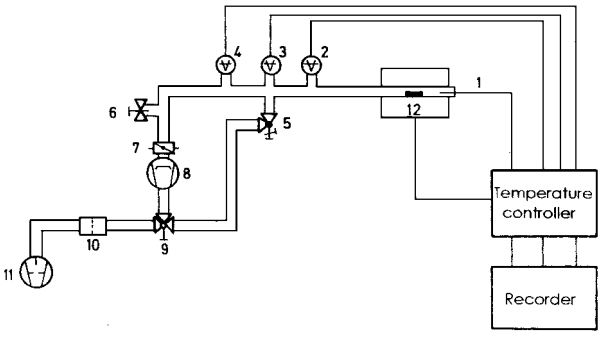

Fig. 1 Experimental controlled rate thermal analysis equipment. 1) Thermocouple, 2) piezoelectric pressure transducer, 3) Penning gauge, 4) Pirani gauge, 5), 6), 7) and 9) valves, 10) alumina tramp, 8) and 11) pumps, 12) furnace.

Results and discussion

Fig. 2 shows the transmission electron micrographs of the goethite samples (G10, G25, and G100) prepared under the conditions described above. All these samples consist of needle-like particles. The size of these particles decreases as the amount of Fe precipitated before the oxidation treatment increases. Thus, the G10 particles are the largest and the G100 the smallest. The specific surface areas as calculated by the single point BET method for the G10, G25, and G100 samples are: 22 m^2 g^{-1}, 43 m^2 g^{-1}, and 95 m^2 g^{-1}, respectively. The X-ray diffraction (XRD) patterns (Fig. 3) of the three solids illustrated in Fig. 2 are characteristic of α-FeOOH. The crystallite size varies with the particle size, so the sizes as calculated from the broadening of the (021) XRD peak are 177 nm, 61 nm, and 32 nm, respectively.

Fig. 4 shows the thermogravimetric curve heated under vacuum at 20 °C min^{-1}, after a previous treatment of the G25 goethite sample at 110 °C for 1 h to remove the hydration water. The weight loss over the range 200–350 °C was 10%, which corresponds to the dehydroxylation of FeOOH according to eqn. (4). The final product of the thermal decomposition of goethite on heating at 350 °C was pure hematite, as illustrated by the XRD pattern of sample G25 after calcination at

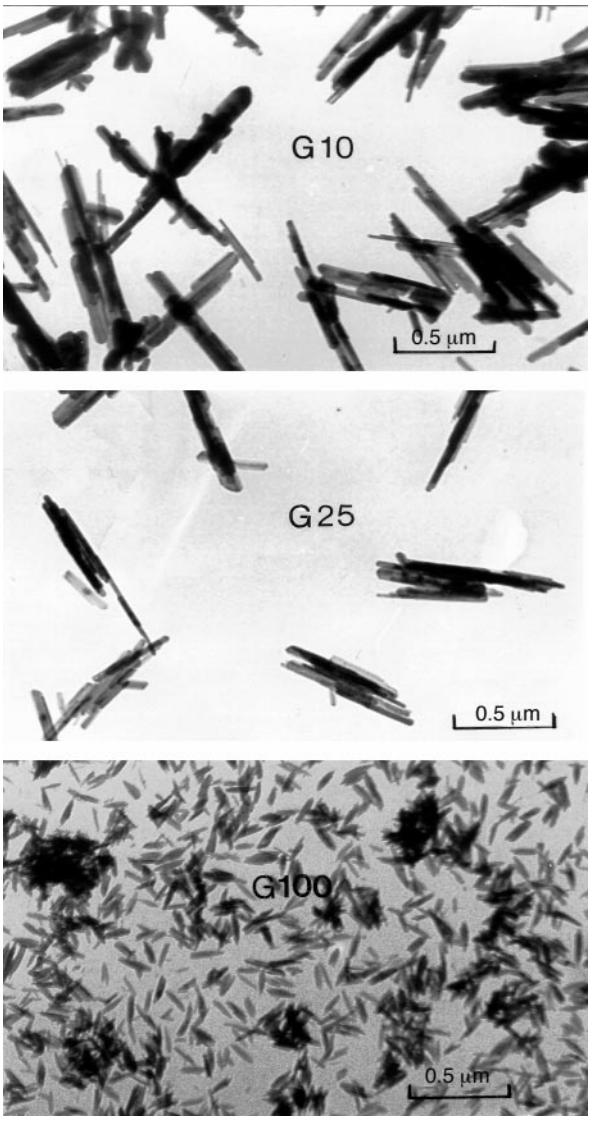

Fig. 2 TEM micrographs of the G10, G25 and G100 goethite samples.

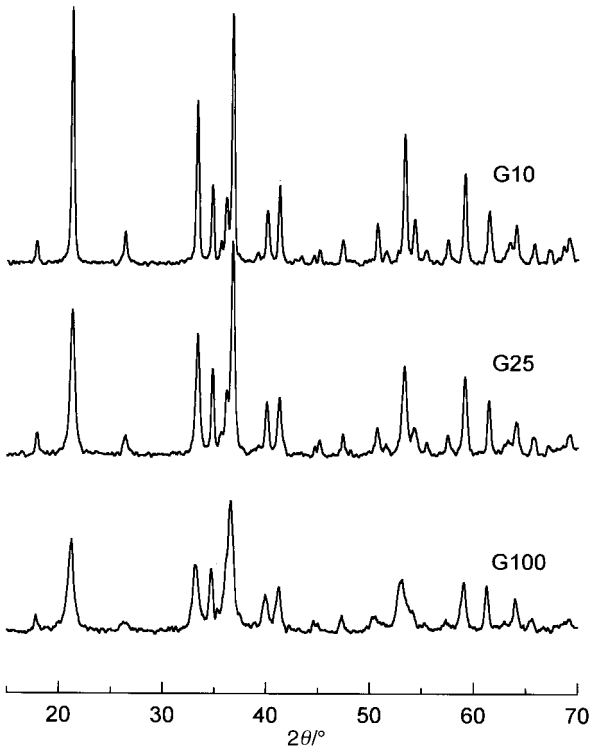

Fig. 3 Powder X-ray diffraction (XRD) patterns of the G10, G25 and G100 goethite samples.

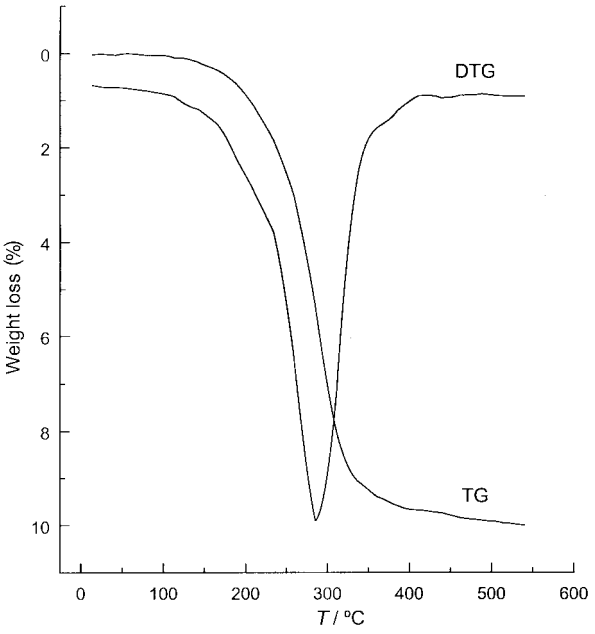

Fig. 4 Thermogravimetric curve of the G25 goethite sample heated under vacuum at 20 °C min^{-1}, after a previous treatment at 110 °C for 1 h to remove the hydration water.

350 °C for 1 h under vacuum (Fig. 5). In addition, no changes were observed in the shape and size of the particles during the thermal treatment, as expected for a topotactic reaction.[15,22,27]

The values of the specific surface area for the α-Fe_2O_3 samples obtained from the thermal decomposition of the G25 goethite sample at a linear heating rate under different experimental conditions are given in Table 1. In all these experiments, the temperature was increased to 350 °C and maintained at this value for 1 h. The TEM micrographs (Fig. 6) of the resulting samples show that the solids with higher specific surface areas exhibit slit-shaped micropores along the longest dimension of the particles. It has been reported from electron

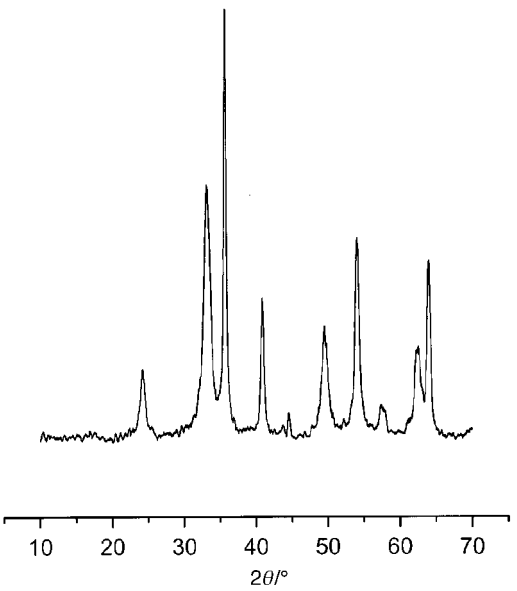

Fig. 5 XRD pattern of the G25 goethite sample calcined under vacuum at 350 °C for 1 h.

Table 1 Specific surface areas of the hematite samples prepared by decomposition of the goethite sample G25 at a linear heating rate

Atmosphere	Heating rate	Specific surface area/m^2 g^{-1}	Sample no.
Vacuum	0.5	83	1
	20	101	2
Static air	0.5	101	3
	20	77	4
	∞^a	56	5
Closed tube	∞^b	49	6

[a]The sample was introduced directly into the furnace at 350 °C. [b]The sample was introduced into a closed tube, so the water pressure over it during the dehydroxylation was $\approx 8 \times 10^3$ Torr.

diffraction data of acicular microcrystals of α-Fe_2O_3 that the elongated direction of the microcrystal is perpendicular to the *c* axis.[28] Thus, the slit shaped pores (Fig. 6A) open along an axis perpendicular to *c*. On the other hand, the sample with the lowest specific surface area has isolated circular pores (Fig. 6C). A similar relation between specific surface area and porosity has been described elsewhere.[15]

The effect of the heating rate on the porosity is different for the experiments carried out in vacuum and in static air. Therefore, in vacuum an increase in the heating rate produces an increase in the specific surface area, whereas in static air the effect is the opposite. It is difficult to give an explanation for this behaviour based only on the linear heating rate results. In principle it would be expected that the developed porosity depends on both the decomposition rate of the precursor and the partial pressure exerted in the close vicinity of the sample by the water vapour generated in the reaction. These two factors would depend on the heating rate and the atmosphere surrounding the sample at the beginning of the experiment; the evolution of this atmosphere can be influenced by the heating rate selected. Therefore, it would be interesting to carry out a careful analysis of the influence of the decomposition rate and the partial pressure of water vapour on the texture of α-Fe_2O_3 obtained from the thermal decomposition of goethite. Constant rate thermal analysis (CRTA) is a suitable method for this purpose.

A plot of the evolution of the temperature and partial pressure of water vapour recorded, using CRTA, as a function of time for the decomposition of the G25 goethite sample under a

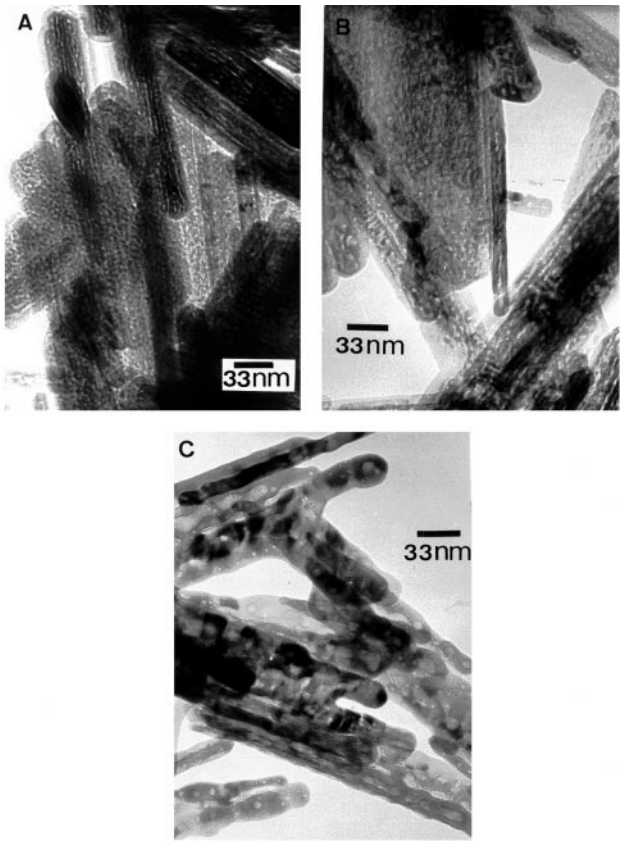

Fig. 6 TEM micrographs of hematite samples 3 (A), 4 (B), and 6 (C) in Table 1, obtained from the G25 goethite sample at a linear heating rate.

constant pressure $P=5.5\times10^{-5}$ mbar and a decomposition rate $C=6.5\times10^{-4}$ min^{-1} is shown as an example in Fig. 7. Fig. 8 includes the reacted fraction (α) values, as calculated from the integral of the pressure curve between the initial and actual point and divided by the total area, as a function of the temperature (T) for three experiments carried out at different decomposition rates. The α–T plots obtained for two CRTA experiments performed at the same reaction rate but at different partial pressures

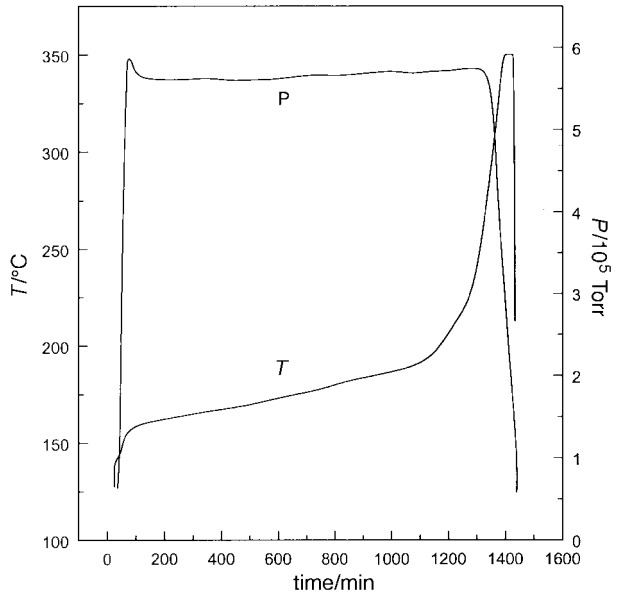

Fig. 7 A plot of the evolution of the temperature and partial pressure of water vapor recorded (using CRTA) as a function of time for the decomposition of the G25 goethite sample under a constant pressure $P=5.5\times10^{-5}$ mbar and a decomposition rate $C=6.5\times10^{-4}$ min^{-1}.

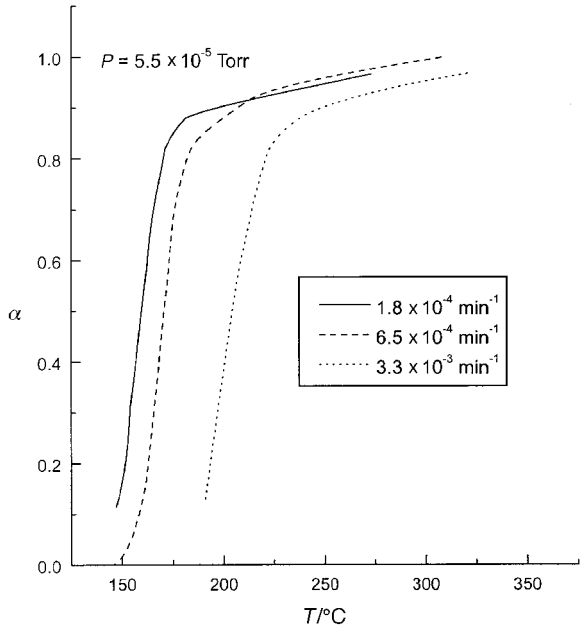

Fig. 8 Reacted fraction (α) as a function of the temperature (T) for three CRTA experiments carried out at the same pressure, 5.5×10^{-5} Torr, and three different reaction rates: 1.8×10^{-4}, 6.5×10^{-4}, and 3.3×10^{-3} min^{-1}.

are included in Fig. 9. Fig. 8 and 9 illustrate how the temperature ranges at which the decomposition takes place depend on the conditions selected by the user. For the experiments carried out at the same water vapour pressure, the lower the decomposition rate, the lower the temperature range of the reaction. This behaviour can be easily understood if we take into account[29] that the rate of a solid state reaction can be described by the general equation

$$\frac{d\alpha}{dt}=Ae^{-E/RT}f(\alpha) \qquad (4)$$

where α is the reacted fraction at time t; A is the Arrhenius preexponential factor; E is the activation energy; T is the absolute temperature; and $f(\alpha)$ is a monotonic function

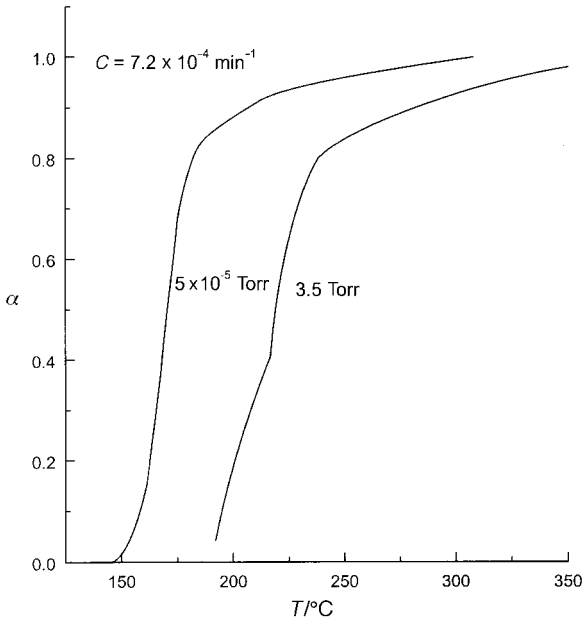

Fig. 9 Reacted fraction (α) as a function of the temperature (T) for two CRTA experiments carried out at the same reaction rate, 7.0×10^{-4} min^{-1}, and two different control pressures 5.5×10^{-5} and 3.7 Torr.

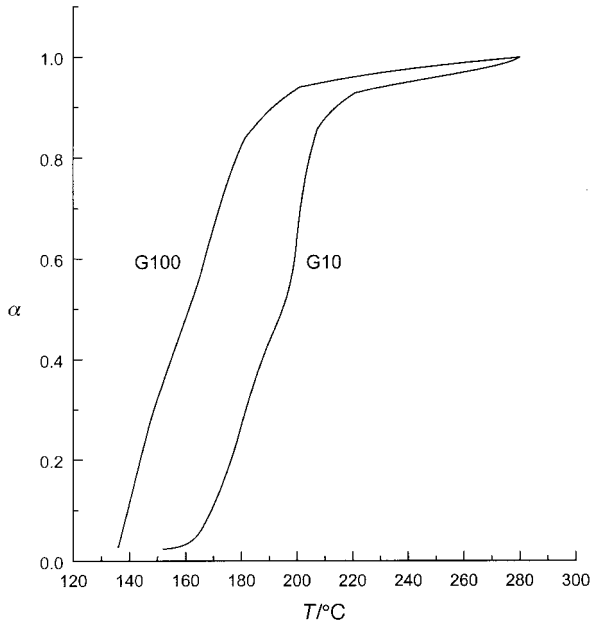

Fig. 10 Reacted fraction (α) as a function of the temperature (T) for the decomposition at constant rate of G10 and G100 goethite samples carried out at a reaction rate of 3.9×10^{-4} min^{-1} and a partial pressure of 5.5×10^{-5} Torr.

depending on the kinetic law obeyed by the reaction whose absolute value increases with increasing α. If the process is carried out at a constant reaction rate $C=\mathrm{d}\alpha/\mathrm{d}t$, eqn. (4) can be written in the form:

$$C=Ae^{-E/RT}\mathrm{f}(\alpha) \qquad (5)$$

Thus, the higher the value of C, the higher must be the temperature at which a particular value of α is reached, provided that eqn. (5) must be fulfilled.

The influence of the partial pressure of water vapour on the thermal decomposition of α-FeOOH is shown in Fig. 9. This figure represents two α–T plots recorded at a constant decomposition rate $C=7.0\times10^{-4}$ min^{-1} but at different selected values for the water vapour pressure produced in the reaction. It can be observed that for the experiment performed at $P=5.5\times10^{-5}$ Torr the temperature range is almost 50 °C lower than that at 3.5 Torr. In order to eliminate the possible effects of different mean decomposition temperature for the different decomposition rates and pressures chosen, on completion of the reaction the temperature of the sample was increased to 350 °C and held for 1 h under high vacuum before cooling. This normalised thermal treatment would make sure that the differences in texture and morphology of the hematite samples obtained as the final product of the thermal decomposition of goethite are due to the experimental conditions used for decomposing the precursor rather than to the thermal treatment undergone by the samples.

Note the low temperature range at which goethite dehydroxylation occurs under a constant pressure of 5.5×10^{-5} mbar and at $C=1.8\times10^{-4}$ min^{-1} (Fig. 8) as compared to the values obtained at a constant heating rate $\beta=20$ °C min^{-1} (Fig. 4). This behaviour is related to the different experimental conditions used. The dehydroxylation rate and the partial pressure of water vapour generated in the vicinity of the sample must be considerably larger in the latter case.

Several authors have reported that pure goethite dehydrates in two steps.[25,30–32] Different explanations have been proposed for this behaviour. Schwertmann[32] established a relation

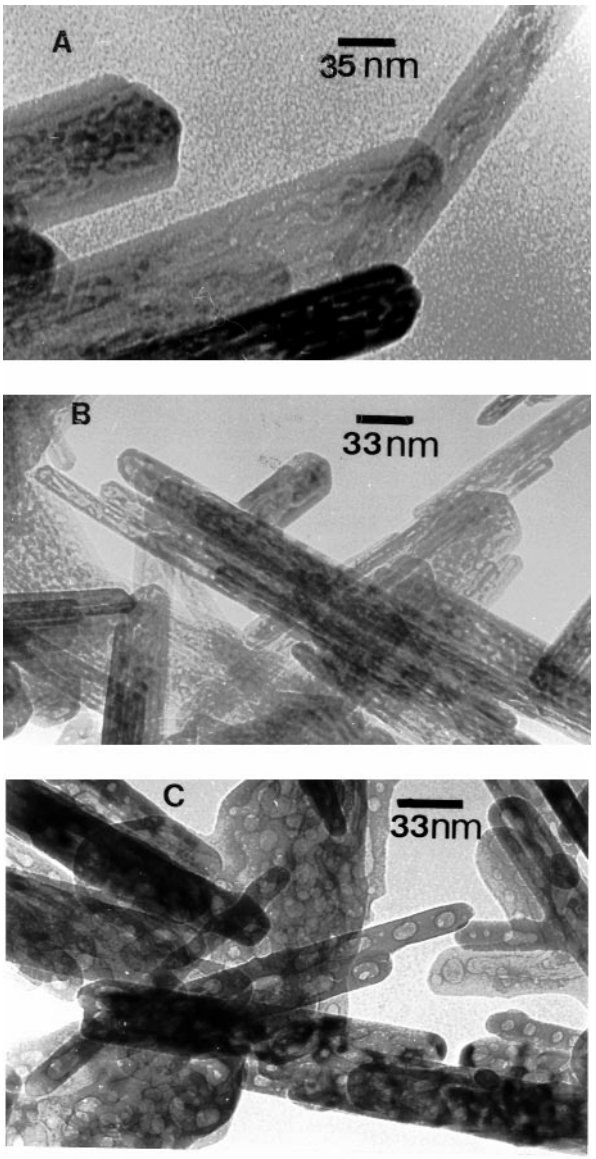

Fig. 11 TEM micrographs corresponding to hematite samples 7 (A), 11 (B), and 13 (C) in Table 2 obtained from CRTA experiments.

Table 2 Specific surface areas and crystallite sizes for the hematite samples prepared by decomposition of the G25 goethite sample by CRTA

Control pressure/Torr	Reaction rate/min^{-1}	Specific surface area/m^2 g^{-1}	Crystallite size		Sample no.
			d_{104}/nm	d_{110}/nm	
5.5×10^{-5}	3.3×10^{-3}	102	8	34	7
	6.5×10^{-4}	89	—	—	8
	2.2×10^{-4}	76	—	—	9
	1.8×10^{-4}	45	—	—	10
3.7	3.0×10^{-3}	83	10	34	11
	7.0×10^{-4}	58	—	—	12
8.2	7.6×10^{-4}	44	12	34	13

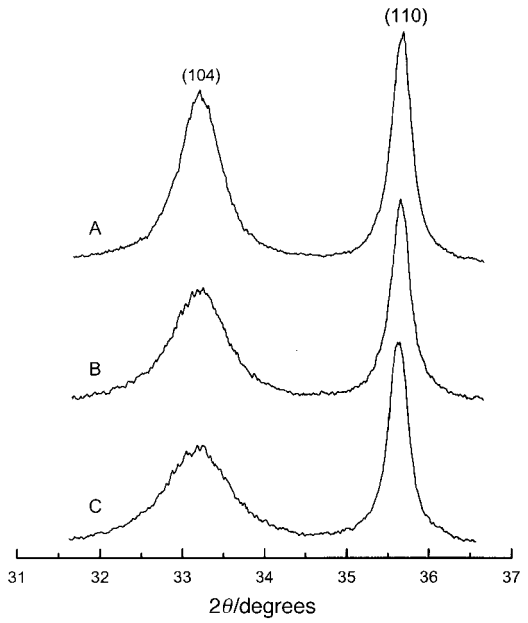

Fig. 12 XRD patterns for the (110) and (104) peaks of hematite samples 13 (A), 11 (B), and 7 (C) in Table 2 obtained from CRTA experiments.

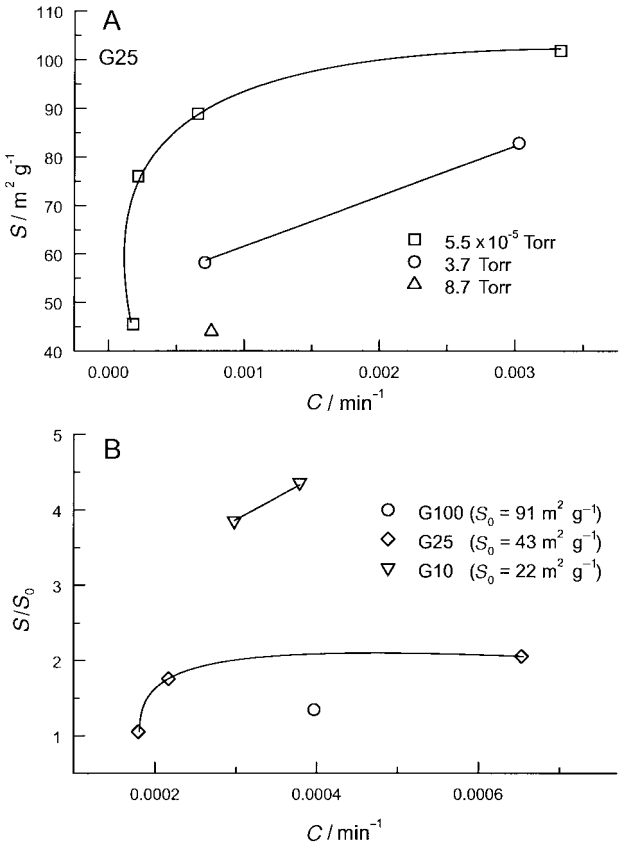

Fig. 13 Specific surface area of the hematite samples as a function of the reaction rate at different pressures (A). Ratios between the specific surface area of the hematite samples, S, and the specific surface area of the goethite precursors, S_0, as a function of the decomposition rate for different goethite precursors (B).

between crystallinity and the two-step decomposition profile, indicating that two steps were observed for highly crystalline goethite samples. Derie *et al.*[31] observed two decomposition steps for high surface area samples. Goss[25] related the two steps to the presence of excess water. It has been reported in the present paper that the same sample decomposed under different conditions yields either a two-step decomposition profile or a single-step one, depending on the experimental conditions. Thus, Fig. 8 and 9 show that at the higher water vapour pressure used, 3.5 mbar, two steps were observed, while at the lower pressure of 5.5×10^{-5} mbar, a single step was observed in the whole range of constant decomposition rates, C, investigated. It was also noticed that the particle size has a significant influence on this behaviour; Fig. 10 shows the α–T plots for two CRTA experiments carried out under identical conditions, but using two different goethite samples. The sample with the largest particles (and the most crystalline), G10, shows two steps, while the other sample, G100, presents only one. The latter behaviour is in agreement with that observed by Schwertmann,[32] which he explained considering the formation of an intermediate in the decomposition of very well crystallised goethite. The results obtained here suggest that the decomposition of α-FeOOH through an intermediate step prior to complete dehydration seems to be strongly dependent on the partial pressure exerted around the sample by the water vapour generated in the reaction. The fact that two steps were observed for the thermal decomposition of the goethite samples with higher particle sizes may perhaps be explained by considering that the water vapour generated inside the particles (because of the thermal decomposition of goethite initiated in inner nuclei) escape less easily as the particle size increases. Thus, the larger the particle size, the higher the partial pressure of water vapour inside the particles. However, careful research into the kinetics of the thermal decomposition of goethite would be necessary to clarify this behaviour.

Table 2 shows the specific surface areas and crystallite sizes of hematite samples obtained by using the CRTA method for decomposing the α-FeOOH. These samples present similar relationships between specific surface area and porosity to those obtained from the thermal decomposition of goethite under a linear heating rate program, as shown in Fig. 11. Taking into consideration the observations of Naono *et al.*[15,16] that the slit-shaped micropores are perpendicular to the c axis, and considering all the intense diffraction peaks recorded for hematite, the (110) peak will give some indication of the dimensions of the crystallites in the direction of the pores and the (104) peak in a direction perpendicular to the pores. Fig. 12 includes the (110) and (104) peaks of the XRD pattern for the three hematite samples with different porosity illustrated in Fig. 11. The (110) peak broadening is not affected by the porosity of the sample, and its profile is identical for all of the samples. On the other hand, the (104) peak is strongly influenced by the porosity of the sample. The crystallite sizes, as calculated from the broadening of these two XRD peaks, are included in Table 2. The dimensions of the crystallites in the (111) direction are identical for all the samples, while the size in the (104) direction varies from 8 to 12 nm for the samples with specific surface areas of 102 and 44 $m^2 g^{-1}$, respectively. It is suggested that the pores perturb the particle structure and act as Bragg domain limits in the c direction according to previous proposals in the literature.[15,22]

The specific surface areas, S, of the hematite samples obtained from the CRTA experiments at different control pressures with the G25 goethite precursor are plotted as a function of the decomposition rate in Fig. 13A. Hematite samples obtained at different vapour pressures under otherwise identical experimental conditions differ widely in their specific surface areas. It can be concluded that the higher the water vapour pressures on the goethite samples the lower the specific surface areas of the oxides. On the other hand, the specific surface area is also affected by the decomposition rate. The decrease in the specific surface area of hematite upon increasing the reaction rate or the partial pressure can be interpreted considering the increase in the temperature range of the decomposition that is produced. Under these conditions, the

mobility of the surface ions may be promoted resulting in faster pore growth and elimination.

Another important parameter in the thermal decomposition of goethite is the particle size of the precursors. Fig. 13B shows a plot of the ratios between the specific areas of the hematite sample, S, and the specific surface areas of the goethite precursors, S_0, as a function of the decomposition rate for the three goethite samples studied here. These results show that the S/S_0 ratio increases upon decreasing the specific surface area of the precursors, and therefore increasing their particle size.

On the other hand, taking into consideration the results obtained from CRTA, it is possible to understand the apparently confusing results concerning the texture of the hematite obtained from the thermal decomposition of goethite under a linear heating rate. Under any particular experimental conditions, an increase in the heating rate, because of kinetic reasons, necessarily leads to an increase in the reaction rate and, according to our previous considerations, to an increase in the specific surface area of hematite produced from goethite. However, the increase in the heating rate could produce an increase in the vapour pressure in the proximity of the sample, and consequently a decrease in the specific surface area of the hematite. For the experiments conducted under vacuum, the increase in the reaction rate is the determining parameter, probably because the pumping minimises the influence of the water vapour. In these experiments an increase in the heating rate produces an increase in the specific surface area. On the other hand, for the experiments in static air, the water vapour pressure has a more significant effect, and hence an increase in the heating rate could produce a decrease in the specific surface area of the hematite. Taking into account that the reaction rate and the partial pressure of water vapour work in opposite directions, it is difficult, if not impossible, to forecast the texture of the final products obtained from the thermal decomposition of goethite without precise control of both experimental parameters. It has been shown that the CRTA method outlined here is a suitable procedure for overcoming this problem.

Conclusions

In summary, the experimental parameters reaction rate and vapour pressure both have a significant influence on the porosity of hematite produced from goethite. Thus, slower reaction rates yield more porous materials than faster ones, whereas an increase in the water vapour pressure produces a decrease in the porosity.

The particle size of the precursors is another important parameter in controlling the porosity. Thus, for the goethite samples composed of particles of different size and decomposed under identical conditions, larger particles yield more porous hematite products.

References

1 H.-T. Sun, C. Cantalini, M. Faccio, M. Pelino, M. Catalano and L. Tapfer, *J. Am. Ceram. Soc.*, 1996, **79**, 927.
2 C. Cantalini and M. Pelino, *J. Am. Ceram. Soc.*, 1992, **75**, 546.
3 A. Brown, J. Hargreaves and B. Rijniersce, *Catal. Lett.*, 1998, **53**, 7.
4 H. Randall, R. Doepper and A. Renken, *Ind. Eng. Chem. Res.*, 1997, **36**, 2996.
5 R. M. Cornell and U. Schwertmann, *The Iron Oxides. Structure, Properties, Reactions, Occurrence and Uses*, VCH, Weinhein, 1996.
6 K. Raj and R. Moskovitz, *J. Magn. Magn. Mater.*, 1990, **85**, 233.
7 C. Sestier, D. Sabolovic, D. Geldwerth, M. Moumaris, J. Roger, J.-N. Pons and A. Halbreich, *C. R. Acad. Sci., Ser. III*, 1995, **318**, 1141.
8 C. Sestier, M. F. Dasilva, D. Sabolovic, J. Roger and J. N. Pons, *Electrophoresis*, 1998, **19**, 1220.
9 F. Gazoeau, J. C. Bacri, F. Gendron, R. Perzynsky, Y. L. Raikher, V. I. Stepanov and E. Dubois, *J. Magn. Magn. Mater.*, 1998, **186**, 157.
10 J. L. Dorman and D. Fiorani, *Magnetic properties of fine particles*, North Holland, Amsterdam, 1992.
11 M. P. Sharrok and R. E. Bodnar, *J. Appl. Phys.*, 1985, **57**, 3919.
12 Y. Maeda, *E.C.L. Techn. Publ.*, 1978, **179**, 1.
13 E. Herrero, M. V. Cabañas, V.-R. M., J. L. Martinez and J. M. Gonzalez-Calbet, *Solid State Ionics*, 1997, **101**, 213.
14 M. Ozaki, S. Krathovil, and E. Matijević, *J. Colloid Interface Sci.*, 1984, **107**, 199.
15 H. Naono and R. Fujiwara, *J. Colloid Interface Sci.*, 1980, **73**, 406.
16 H. Naono, K. Nakai, T. Sueyoshi and H. Yagi, *J. Colloid Interface Sci.*, 1987, **120**, 439.
17 M. Pelino, L. Toro, M. Petroni, A. Florindi and C. Cantalini, *J. Mater. Sci.*, 1989, **24**, 409.
18 P. F. Rossi, G. Caracciolo and G. Busca, *Colloids Surf.*, 1988, **32**, 75.
19 J. L. Rendon, J. Cornejo, P. De Arambarri and C. J. Serna, *J. Colloid Interface Sci.*, 1983, **92**, 508.
20 D. Beruto, *Mater. Chem. Phys.*, 1983, **8**, 233.
21 S. Hirokawa, T. Naito and T. Yamaguchi, *J. Colloid Interface Sci.*, 1986, **112**, 268.
22 P. Duvigneud and R. Derie, *J. Solid State Chem.*, 1980, **34**, 323.
23 C. Serna and J. Iglesias, *J. Mater. Sci. Lett.*, 1986, **5**, 901.
24 F. Watari, J. van Landuyrt, P. Delavignette, S. Amelickx and N. Igata, *Phys. Status Solidi A*, 1982, **73**, 215.
25 G. Goss, *Mineral. Mag.*, 1987, **51**, 437.
26 E. Wolska and U. Schwertmann, *Phys. Status Solidi A*, 1989, **114**, K11.
27 L. Volpe and M. Bougart, *Catal. Rev. Sci. Eng.*, 1985, **27**, 515.
28 G. W. van Oosterhout, *Acta Crystallogr.*, 1960, **13**, 932.
29 F. J. Gotor, M. Macías, A. Ortega and J. M. Criado, *Int. J. Chem. Kinet.*, 1998, **30**, 647.
30 A. M. Gadala and T. W. Livingston, *Thermochim. Acta*, 1989, **145**, 1.
31 R. Derie, M. Ghodsi and C. Calvo-Roche, *J. Therm. Anal.*, 1976, **9**, 435.
32 U. Schwertmann, *Thermochim. Acta*, 1984, **78**, 39.

Paper 9/01098J